International Pharmacy Acta. 2025; 8(1): e10
Original Research Article
OPEN ACCESS
ISSN: 2645-3266

Computer-Aided Design of Thiazolone Derivatives Targeting HCV NS5B Allosteric Site Using Molecular Docking, ADME/Tox Profiling, and Dynamics

Mehdi Gueroui[a*], Amina Kerrada[b], Lina Bouden[c], Lina Bouchra Nedjar[c], Manel Boudina[c], Aya Aiech[c]

a. Laboratory of Medicinal Chemistry, Faculty of Medicine of Constantine, Salah Boubnider University Constantine 3, Algeria.
b. Laboratory of Pharmacology, Faculty of Medicine of Constantine, Salah Boubnider University Constantine 3, Algeria.
c. Laboratory of Medicinal Chemistry, Faculty of Medicine of Constantine, Salah Boubnider University Constantine 3, Algeria.

Article Info:
Received: November 2025
Accepted: December 2025
Published online: December 2025

* **Corresponding Author:**
Mehdi Gueroui
Email: mehdi.gueroui@univ-constantine3.dz

ABSTRACT:

Hepatitis C virus (HCV) remains a major health concern, with the NS5B RNA-dependent RNA polymerase representing a crucial target for antiviral drug discovery. This study aimed to identify selective NS5B inhibitors from a library of thiazolone derivatives using an integrated computer-aided drug design workflow. Molecular docking was performed with AutoDock Vina via PyRx on 1000 compounds, and pharmacokinetic and toxicity properties were evaluated using SwissADME and PreADMET. Normal Mode Analysis (NMA) was then applied through the iMODS server to assess the dynamic effects of ligand binding on protein flexibility. Three compounds, CID137131214, CID135435208, and CID2329878, demonstrated strong binding affinities, favorable ADME/Tox profiles, and key interactions with the NS5B allosteric site. Notably, CID135435208 induced a rigidifying effect, supporting its inhibitory potential. These results highlight promising scaffolds for further biological validation and provide a rational framework for the design of novel HCV therapeutics. However, this study is limited by the lack of experimental validation, which will be addressed in future work.

Keywords: HCV; NS5B polymerase; Thiazolone derivatives; Molecular docking; ADME/Tox; Normal mode analysis.

Please Cite this article as: Gueroui M, Kerrada A, Bouden L, Nedjar LB, Boudina M, Aiech A. Computer-Aided Design of Thiazolone Derivatives Targeting HCV NS5B Allosteric Site Using Molecular Docking, ADME/Tox Profiling, and Dynamics. Int. Pharm. Acta. 2025; 8(1):e10.
DOI: https://doi.org/10.22037/ipa.v8i1.50712

1. Introduction

Hepatitis C virus (HCV) remains a major global health problem, responsible for severe hepatic complications including fibrosis, cirrhosis, and hepatocellular carcinoma (Figure 1) [1-4]. Although direct-acting antivirals (DAAs) have considerably improved treatment outcomes, the emergence of resistant viral strains continues to drive the search for new therapeutic agents [5-7].
The RNA-dependent RNA polymerase NS5B plays a pivotal role in HCV replication and has therefore become a key target in antiviral drug development.

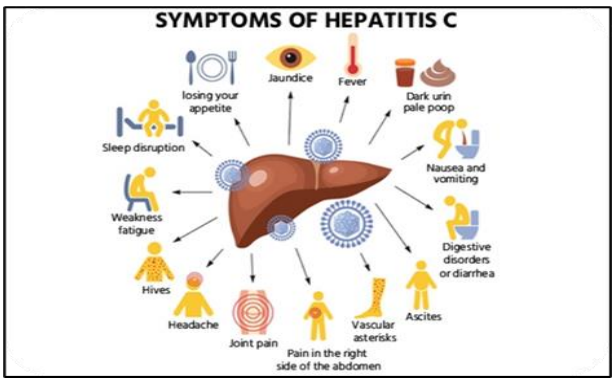

Figure 1. Symptoms associated with Hepatitis C virus infection.

In particular, allosteric inhibitors can modulate polymerase activity while minimizing cross-resistance with existing therapies [8–15].
Thiazolone derivatives have recently attracted attention for their antiviral properties and their interactions with polymerase enzymes. However, their inhibitory potential against the HCV NS5B polymerase has not been comprehensively evaluated, which motivated their Selection in this study.
The present work aims to identify novel NS5B inhibitors using a computer-aided drug design approach. A library of 1000 structurally related thiazolone derivatives was virtually screened using molecular docking, followed by ADME/Tox prediction to assess pharmacokinetic suitability. The most promising candidates were further analyzed using Normal Mode Analysis (NMA) to evaluate their effects on the structural dynamics of NS5B. This integrated workflow provides a rational framework for the discovery of new anti-HCV agents with optimized pharmacological characteristics.

2. Materials & Methods

2.1. **Hardware**

The simulations were performed on a Dell microcomputer equipped with an Intel Core i9 processor, 32 GB of RAM, and Windows 11 Pro.

2.2. Databases, software, and tools used were Protein Data Bank (PDB)

Download of the crystallographic structure of NS5B (PDB ID: 2HWI). **PubChem**: retrieval of structural analogues with a similarity threshold of 83%. A similarity threshold of 83% was applied to retrieve a structurally diverse library of thiazolone derivatives while avoiding compounds already under clinical or preclinical evaluation. This cutoff enabled the construction of a virtual screening library enriched with novel, unexplored analogues suitable for early-stage drug discovery. **Discovery Studio v2021** and **AutoDock Tools 1.5.7**: preparation of the target protein. **Avogadro**: geometric optimization of ligands. **AutoDock Vina v1.2.3** integrated within **PyRx v0.8:** molecular docking simulations. **SwissADME** and **PreADMET (accessed July 2024):** evaluation of ADME/Tox properties [19-20]. **BIOVIA Discovery Studio v2021**: visualization and interaction profiling. **iMODS (accessed July 2024)**: Analysis of protein flexibility using Normal Mode Analysis.

2.3. Molecular docking study [16-17]

2.3.1. Target protein preparation

Removal of water molecules and ions, and addition of missing hydrogens.

2.3.2. Ligand preparation

Generation and optimization of 3D structures for the 1000 selected analogues.

2.3.3. Molecular docking

Calculation of interaction energies and identification of the most stable conformations.
Molecular docking was performed using AutoDock Vina, integrated into PyRx 0.8.
Docking parameters:
Center: x = 8.560, y = 34.308, z = 74.852
Grid box dimensions: x = 40 Å, y = 40 Å, z = 40 Å
Exhaustiveness: 8
Number of generated modes: 9
Protocol validation was performed by redocking the co-crystallized ligand and calculating the RMSD between the resulting pose and the crystallographic structure.

2.3.4 ADME/Tox filtering

Selection of compounds meeting Lipinski's and Veber's rules, Tables 1 and 2.

Table 1: ADME properties summary of the top 10 selected compounds. Bioavailability was 0.55.

CID	GI Absorption	BBE Permeability	P-gp Substrate	Inhibition of Cytochromes P450				
				CYP 1A2	CYP 2C19	CYP 2C9	CYP 2D6	CYP 3A4
135401990	high	-	-	+	+	+	-	-
135435208	high	-	-	+	+	+	-	-
135641010	high	-	-	+	+	+	-	-
137084858	high	-	-	+	+	+	-	-
135403917	high	-	-	+	+	+	-	-
135950057	high	-	-	+	+	+	-	-
135511556	high	-	-	+	+	+	-	-
137172118	high	-	-	+	+	+	-	-
136060628	Low	-	-	+	+	+	-	-
136060631	Low	-	-	+	+	+	-	-
136060630	Low	-	-	+	+	+	-	-

Table 2: Normal Mode Analysis parameters and eigenvalues for unbound NS5B and selected complexes.

Complex	Global Mobility	Eigenvalue (Rigidity)	Effect on the Structure	Correlations (Covariance)
Protein alone	Clear flexible regions	Medium	Moderately mobile structure	Balanced correlations and anti-correlations
CID2329878	Slightly reduced mobility	Low (flexible)	Local stabilization	Locally reinforced correlations
CID135435208	Strongly reduced mobility	High (rigid)	Significant rigidification	Long-range correlations and anti-correlations
CID137131214	Similar to protein alone	Medium	Negligible impact	Few changes

2.3.5. Interaction visualization

Analysis of hydrogen bonds and hydrophobic interactions between the ligands and NS5B.

2.4. Normal mode dynamics study

The conformational dynamics of the protein alone and in complex with three ligands identified through molecular docking (CID2329878, CID135435208, and CID137131214) were evaluated using the iMODS server (https://imods.iqfr.csic.es/). This approach relies on normal mode analysis (NMA), which predicts the protein's accessible collective motions at low energetic cost. The parameters analyzed included theoretical B-factors, deformability profiles, eigenvalues associated with the normal modes, and covariance maps of residual movements.

3. Results & Discussion

3.1. Docking protocol validation

An excellent overlap was observed between the co-crystallized ligand (red) and the best pose predicted by AutoDock Vina (green). The root-mean-square deviation (RMSD) between these two conformations was 1.154 Å, well below the commonly accepted threshold of 2 Å for docking protocol validation. This result confirms the reliability and accuracy of the implemented protocol (Figure 2).

3.2. Selection of the best inhibitors

Following the molecular docking screening of the chemical library, compounds exhibiting interaction energies lower than that of the native ligand were identified. From these, 22 inhibitors were selected, showing binding energies (ΔG) equal to or lower than -9.0 kcal/mol. These results suggest a higher binding affinity than that of the reference ligand. The interaction energies and identifiers of the selected compounds are summarized in Table 3.
To contextualize the docking results, the binding energies of the top thiazolone derivatives were compared with that of the native reference ligand sofosbuvir, which yielded an affinity of –8.7 kcal/mol under the same docking conditions. The best-performing compounds identified in this study displayed comparable or better scores, supporting their potential relevance as NS5B inhibitors (Figure 3-4).

3.3. Analysis of ligand-target interactions

The reference ligand and the three best candidates selected after ADME/Tox filtering were re-docked into the active site of NS5B, and their interactions were visualized using Biovia Discovery Studio (Figure 5).

3.4. Analysis of ligand–target interactions

Visualization of the binding modes of the 10 best candidate ligands within the allosteric site of the target protein, and Analysis of their established interactions, confirmed their high selectivity.

Figure 2. Symptoms associated with Hepatitis C virus infection.

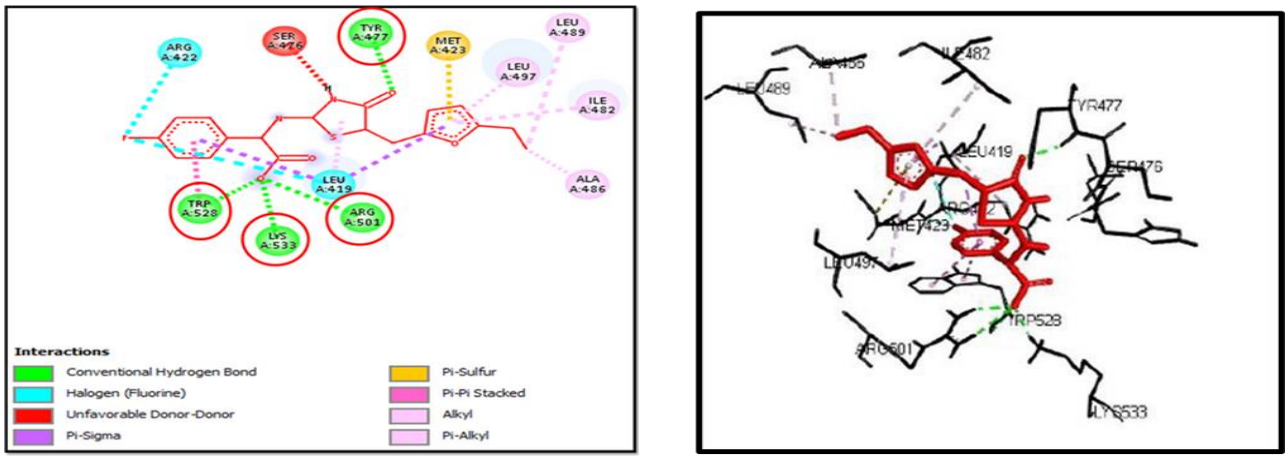

Figure 3. 2D and 3D interaction diagrams of the native ligand with NS5B.

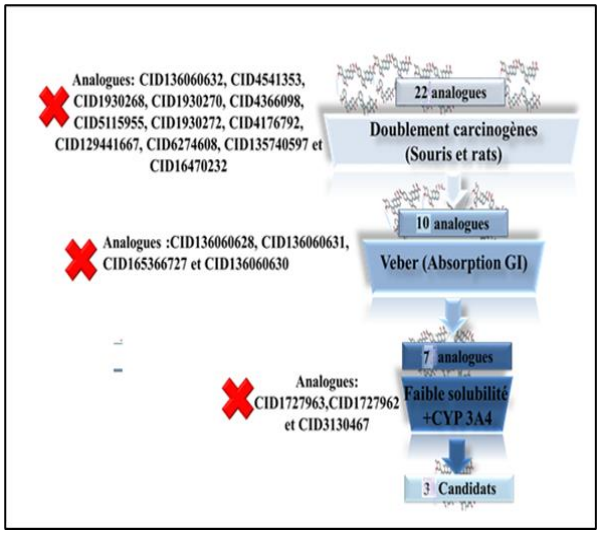

Figure 4. ADME/Tox filtering process applied to the 22 top-scoring compounds.

Key observations include: Among the hydrogen bonds, the one involving Arg501 was the most frequently observed. A consistent hydrogen bond was formed between the thiazolone ring oxygen atom and the protein in all complexes. Hydrophobic interactions involving the aromatic rings of the ligands were constantly present. The most conserved among these were: π-π interactions with Trp528, and π-sigma interactions with Leu419.
The recurrence of these interactions suggests that they play a critical role in stabilizing the complexes within the active site. Additionally, their consistent presence raises the hypothesis of a potential contribution to the biological activity of the ligands.

3.5. Normal mode analysis study

The Analysis of the protein's intrinsic conformational dynamics, performed using Normal Mode Analysis (NMA), assessed the effects of the ligands CID2329878, CID135435208, and CID137131214 on the protein's flexibility and collective motions. This approach provided complementary insights into the stability of the formed complexes and the potential influence of these ligands on the functional dynamics of the target protein.

Table 3: Binding free energy (ΔG, kcal/mol) of top 22 compounds obtained through molecular docking.

	CID	Energy
Native ligand	**135401990**	**-8.7**
1	136060632	-10.0
2	136060628	-9.8
3	136060631	-9.8
4	4541353	-9.7
5	165366727	-9.6
6	137131214	-9.6
7	135435208	-9.3
8	1930268	-9.2
9	1930270	-9.2
10	136060630	-9.2
11	4366098	-9.2
12	5115955	-9.2
13	1727963	-9.2
14	1930272	-9.1
15	4176792	-9.1
16	129441667	-9.1
17	1727962	-9.1
18	3130467	-9.1
19	6274608	-9.1
20	16470232	-9.0
21	135592479	-8.9
22	136354474	-8.9

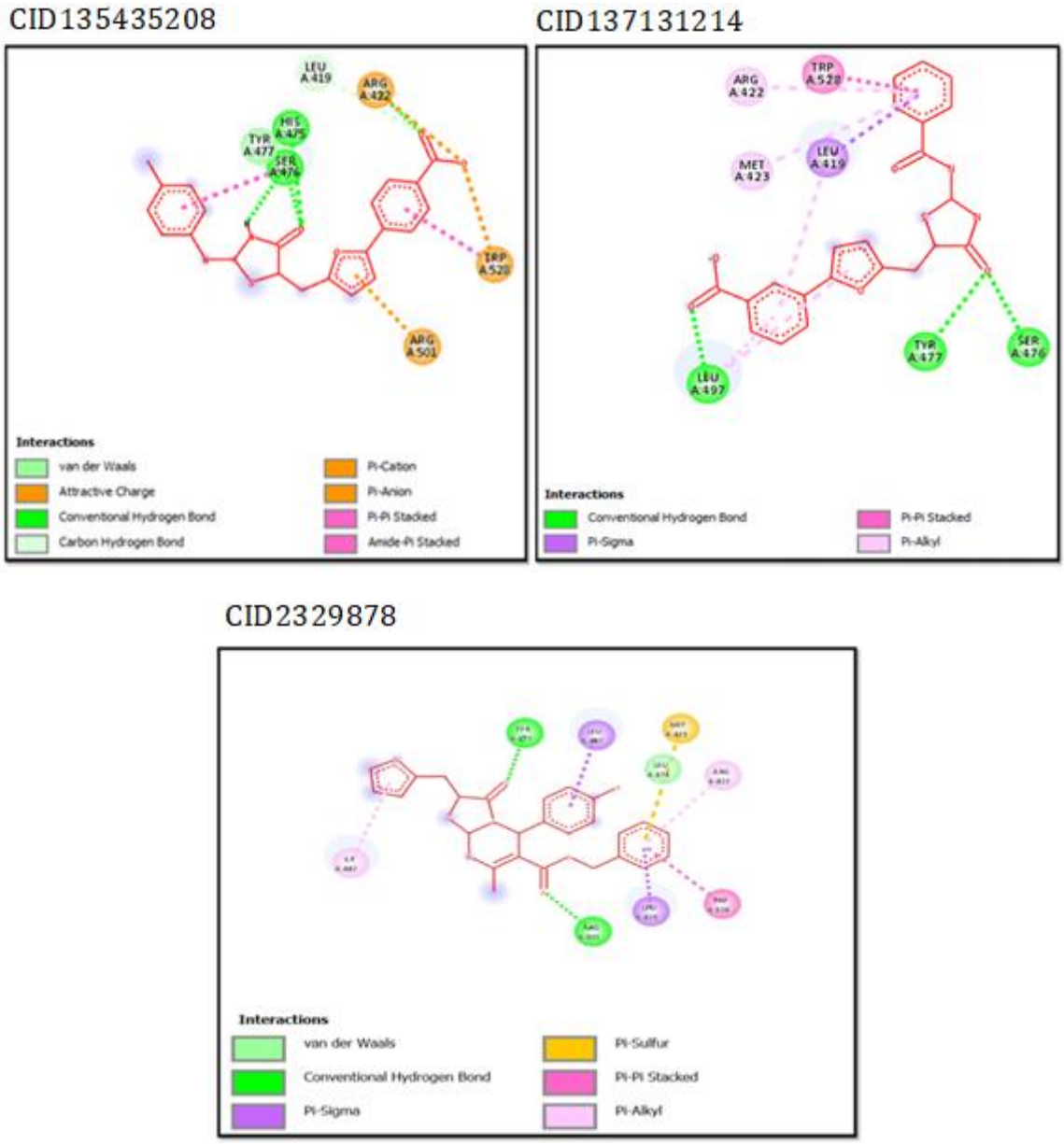

Figure 5. 2D interaction diagrams of CID137131214, CID135435208, and CID2329878 with NS5B.

3.5.1. Deformability and Theoretical B-Factors

The deformability profiles reveal localized peaks corresponding to more flexible regions within the polypeptide chain. These peaks remain relatively constant between the apo form and its ligand-bound complexes, indicating that ligand binding does not induce major alterations in local flexibility. However, minor amplitude variations are observed in certain regions, suggesting local stabilization of specific residues upon ligand binding.
The simulated B-factors show good agreement with the experimental values obtained from the PDB file. A slight reduction in peak amplitudes is observed in the complexes, suggesting that the ligand-protein interactions generally rigidify the protein structure, especially in certain functional or allosteric regions.

3.5.2. Eigenvalues and cumulative variance

The eigenvalues associated with the normal modes reflect the magnitude of the molecular motions. For all three systems, the first eigenvalue is almost identical (e.g., 2.58E-04), indicating that the dominant collective motions are conserved.

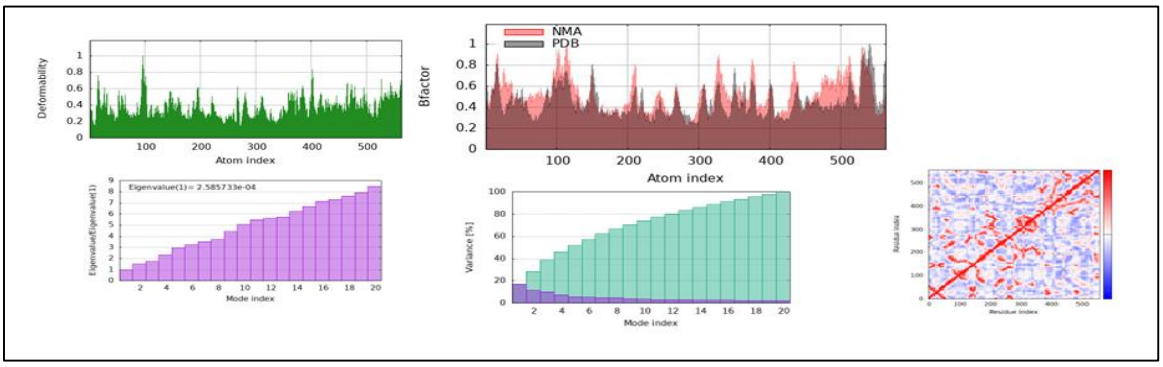

Figure 6. Normal Mode Analysis of unbound NS5B.

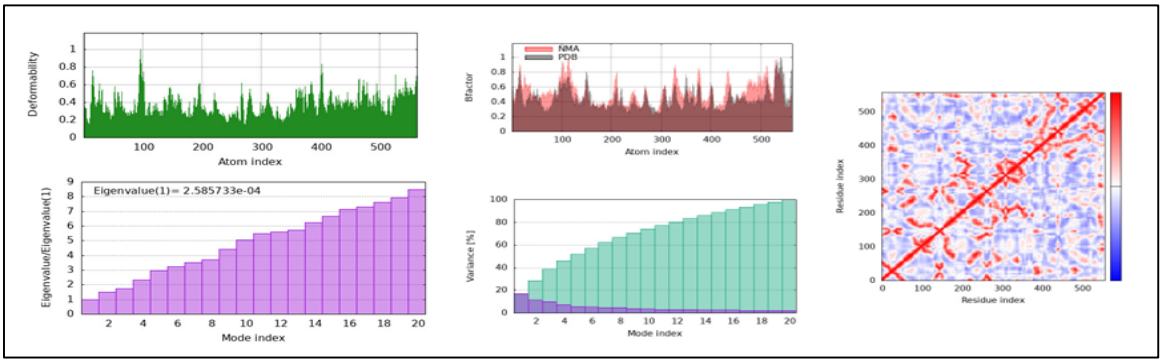

Figure 7. Normal Mode Analysis of NS5B complexed with CID2329878.

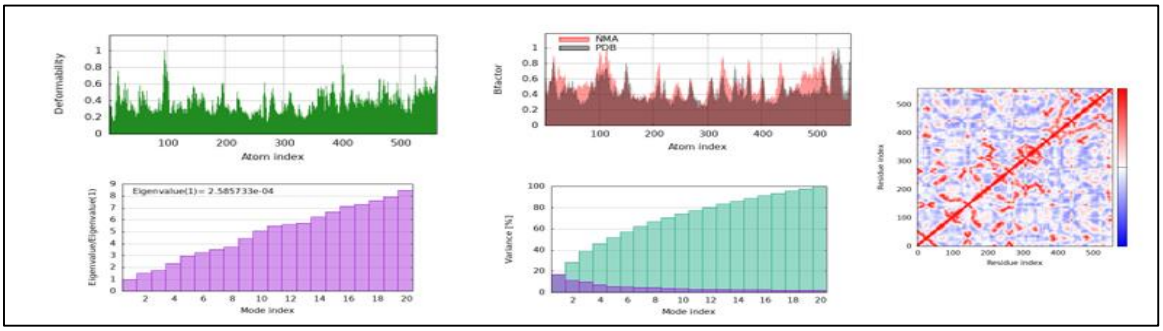

Figure 8. Normal Mode Analysis of NS5B complexed with CID135435208.

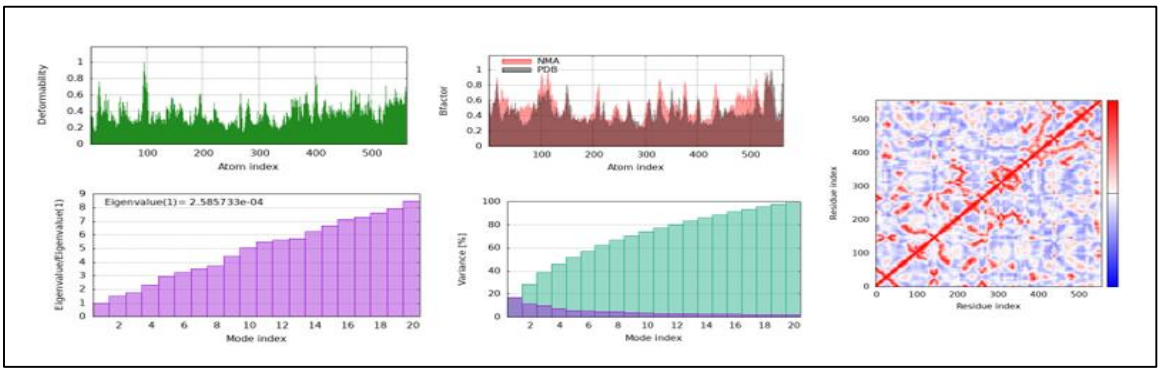

Figure 9. Normal Mode Analysis of NS5B complexed with CID137131214.

However, slight differences in the order and relative intensity of the modes reflect subtle modulations of global dynamics induced by the ligands.
The cumulative variance indicates that the first 10-15 modes account for more than 80% of the total variance, a distribution typical of biological systems. This suggests that the most significant motions are concentrated in a few dominant modes. A slight increase in the variance captured by the first modes in the complexes indicates a reduction in dynamic complexity, possibly related to a more constrained, stabilized conformation.

3.5.3 Dynamical cross-correlation maps (DCCM)

The DCCM maps display the correlations of atomic displacements between residue pairs. In the apo form, strongly correlated regions (in red) are visible, reflecting the collective motions typically associated with functional activity.
In ligand-bound complexes, these correlated regions are altered or weakened, particularly in the protein's central or peripheral regions, suggesting that ligand binding modifies internal communication pathways within the protein and could impact its biological function.

3.5.4 Dynamic interpretation

The NMA results indicate that ligand binding can significantly modulate the molecular dynamics of the target protein (Figures 6-9). CID135435208 notably rigidifies the protein structure, potentially enhancing conformational stability and thereby favoring more efficient inhibition. CID2329878, on the other hand, appears to facilitate slightly more movements, which might be beneficial in an allosteric regulation context. CID137131214 shows an almost unchanged dynamic profile, suggesting a weaker or less structurally influential interaction.
These findings complement the molecular docking results, providing a dynamic perspective on the ligand-protein interactions, which are crucial in rational drug design.

4. Conclusion

This in silico investigation led to the identification of three promising thiazolone derivatives, CID137131214, CID135435208, and CID2329878, as potential selective inhibitors of the hepatitis C virus NS5B RNA polymerase. Through an integrated computer-aided drug design workflow combining virtual screening, molecular docking, ADME/Tox prediction, and Normal Mode Analysis (NMA), these compounds demonstrated strong binding affinities, favorable pharmacokinetic and toxicity profiles, and relevant dynamic effects on the target protein. The NMA-based flexibility analysis provided complementary insights into the structural and functional consequences of ligand binding, highlighting conformational stabilization consistent with the ligand's inhibitory potential. These findings strongly support the selected compounds as starting points for the development of novel anti-HCV agents. However, the present study is limited to computational predictions. Future work will require experimental validation, including NS5B enzymatic inhibition assays, cytotoxicity evaluation, and long-timescale molecular dynamics simulations, to confirm the therapeutic potential of these compounds and advance them toward preclinical development.

Acknowledgements

The author thanks all the people who participated in this study.

Conflict of interest

There is no conflict of interest.

Funding

This study received no specific grant from any funding agency in the public, commercial, or not-for-profit sectors.

Authors' ORCIDs

Mehdi Gueroui:
https://orcid.org/0000-0002-9789-421X
Amina Kerrada:
https://orcid.org/0009-0001-0875-243X

References

1. Kim A. Hepatitis C Virus. Ann Intern Med. 6 Sept 2016;165(5): ITC33 48.
2. Taha G, Ezra L, Abu-Freha N. Hepatitis C Elimination: Opportunities and Challenges in 2023. Viruses. juill 2023;15(7):1413.
3. Tohme RA, Holmberg SD. Is sexual contact a major mode of hepatitis C virus transmission? Hepatology. 2010;52(4):1497 505.
4. Lonardo A, Adinolfi LE, Restivo L, Ballestri S, Romagnoli D, Baldelli E, et al. Pathogenesis and significance of hepatitis C virus steatosis: An update on survival strategy of a successful pathogen. World J Gastroenterol. 21 juin 2014;20(23):7089 103.
5. Bassani D, Moro S. Past, Present, and Future Perspectives on Computer-Aided Drug Design Methodologies. Molecules. janv 2023;28(9):3906.
6. Dudareva S, Faber M, Zimmermann R, Bock CT, Offergeld R, Steffen G, et al. Epidemiologie der Virushepatitiden A bis E in Deutschland. Bundesgesundheitsbl. 1 févr 2022;65(2):149 58.
7. Rossi LMG, Escobar-Gutierrez A, Rahal P. Advanced Molecular Surveillance of Hepatitis C Virus. Viruses. mars 2015;7(3):1153 88.
8. Shepard CW, Finelli L, Alter MJ. Global epidemiology of hepatitis C virus infection. The Lancet Infectious Diseases. 1 sept 2005;5(9):558 67.
9. Couroucé AM. De l'hépatite non-A non-B à l'hépatite C. Transfusion Clinique et Biologique. 1 janv 1997;4(3):287 90.
10. El-Kassas M, Awad A. Metabolic aspects of hepatitis C virus. World J Gastroenterol. 14 juin 2022;28(22):2429 36.

11. Chigbu DI, Loonawat R, Sehgal M, Patel D, Jain P. Hepatitis C Virus Infection: Host–Virus Interaction and Mechanisms of Viral Persistence. Cells. 25 avr 2019;8(4):376.
12. Jafri S, Gordon SC. Epidemiology of Hepatitis C. Clinical Liver Disease. déc 2018;12(5):140 2.
13. Mohd Hanafiah K, Groeger J, Flaxman AD, Wiersma ST. Global epidemiology of hepatitis C virus infection: New estimates of age-specific antibody to HCV seroprevalence. Hepatology. 2013;57(4):1333 42.
14. Gower E, Estes C, Blach S, Razavi-Shearer K, Razavi H. Global epidemiology and genotype distribution of the hepatitis C virus infection. J Hepatol. nov 2014;61(1 Suppl):S45-57.
15. Chevaliez S, Pawlotsky JM. Hepatitis C Virus Serologic and Virologic Tests and Clinical Diagnosis of HCV-Related Liver Disease. International Journal of Medical Sciences. 1 avr 2006;3(2):35 40.
16. Agu PC, Afiukwa CA, Orji OU, Ezeh EM, Ofoke IH, Ogbu CO, et al. Molecular docking as a tool for the discovery of molecular targets of nutraceuticals in diseases management. Sci Rep. 17 août 2023;13(1):13398.
17. Fadlan A, Nusantoro YR. The Effect of Energy Minimization on The Molecular Docking of Acetone-Based Oxindole Derivatives. JKPK (Jurnal Kimia dan Pendidikan Kimia). 30 avr 2021;6(1):69 77.
18. Jain R. Review on Computational Bioinformatics and Molecular Modelling: Novel Tool for Drug Discovery. International Journal of Trend in Scientific Research and Development. 31 déc 2018;Volume-3:51 6.
19. Veber DF, Johnson SR, Cheng HY, Smith BR, Ward KW, Kopple KD. Molecular Properties That Influence the Oral Bioavailability of Drug Candidates. J Med Chem. 1 juin 2002;45(12):2615 23.
20. Kamiya Y, Handa K, Miura T, Yanagi M, Shigeta K, Hina S, et al. In Silico Prediction of Input Parameters for Simplified Physiologically Based Pharmacokinetic Models for Estimating Plasma, Liver, and Kidney Exposures in Rats after Oral Doses of 246 Disparate Chemicals. Chem Res Toxicol. 15 févr 2021;34(2):507 13.